

Accepted Manuscript

Organic overloading affects the microbial interactions during anaerobic digestion in sewage sludge reactors

Guilherme H.R. Braz, Nuria Fernandez-Gonzalez, Juan M. Lema, Marta Carballa



PII: S0045-6535(19)30117-1

DOI: <https://doi.org/10.1016/j.chemosphere.2019.01.124>

Reference: CHEM 23039

To appear in: *ECSN*

Received Date: 3 September 2018

Revised Date: 21 November 2018

Accepted Date: 19 January 2019

Please cite this article as: Braz, G.H.R., Fernandez-Gonzalez, N., Lema, J.M., Carballa, M., Organic overloading affects the microbial interactions during anaerobic digestion in sewage sludge reactors, *Chemosphere* (2019), doi: <https://doi.org/10.1016/j.chemosphere.2019.01.124>.

This is a PDF file of an unedited manuscript that has been accepted for publication. As a service to our customers we are providing this early version of the manuscript. The manuscript will undergo copyediting, typesetting, and review of the resulting proof before it is published in its final form. Please note that during the production process errors may be discovered which could affect the content, and all legal disclaimers that apply to the journal pertain.

**Organic overloading affects the microbial interactions during
anaerobic digestion in sewage sludge reactors**

Guilherme H. R. Braz^a, Nuria Fernandez-Gonzalez^{a*}, Juan M. Lema^a, Marta Carballa^a

Submitted to:

Chemosphere

^a Department of Chemical Engineering, Institute of Technology, Universidade de Santiago de Compostela, Constantino Candeira s/n, 15782 Santiago de Compostela, Galicia, Spain

e-mail addresses:

G.H.R.B.: guilhermehenrique.rodriguesbraz@rai.usc.es

N.F-G.: *** Corresponding author.** e-mail: nuria.fernandez@usc.es

phone: +34 881 816 019

J. M. L.: juan.lema@usc.es

M. C.: marta.carballa@usc.es

1 Abstract

2 There is still a lack of information about microbial interactions of anaerobic digestion
3 microbiome during process disturbance what impedes to predict the mechanisms that
4 drive community dynamics on these events. This paper aims to determine how an
5 organic overloading affects these interactions and to characterize in detail the
6 microbiome structure and diversity in sewage sludge anaerobic reactors during an
7 acidosis event. Two identical sewage sludge anaerobic reactors were subjected to an
8 organic loading shock by adding glycerol waste. As consequence, volatile fatty acids
9 accumulated after only 24 hours (up to 2.5 g/L) while *Bacteroidales* and
10 *Methanomicrobiales* became displaced by *Firmicutes* and *Methanosaeta* sp, showing
11 that reactor acidosis can occur without an immediate decline of this methanogen.
12 Network analysis revealed 9 clusters of co-occurring microorganisms with different
13 behaviors during overloading. At first, *Veillonellaceae* family, the main glycerol
14 degrading, associated with *Candidatus Cloacimonetes*, volatile fatty acids fermenters,
15 increased their relative abundance in detriment of the syntrophic bacteria; although as
16 conditions become more acidic, these groups were displaced by other fermenters like
17 *Porphyromonadaceae* and *Chitinophagaceae*. Eventually, the methanogenesis failed
18 h after organic overloading, when pH reached values lower than 6. Overall, our results
19 showed a succession of functionally redundant microorganisms, most likely because of
20 niche specialization during organic overloading. The detailed temporal analysis
21 elucidated the processes governing the dynamics anaerobic digestion microbiome, a
22 knowledge required to develop anaerobic digestion management strategies based on its
23 microbiome during process disturbances.

24 Keywords

25 Anaerobic microbiome; glycerol; *Methanosaeta*; sludge digestion; *Veillonellaceae*.

26 1. Introduction

27 Anaerobic digestion (AD) is a biological process governed by a complex
28 consortium of microorganisms that works symbiotically to degrade organic matter into
29 methane, water and carbon dioxide. The variability of AD microbial community is often
30 related with AD performance (De Vrieze et al., 2013). Hence, knowledge about the
31 structural organization and functioning of these communities, especially during AD
32 imbalance events, is essential to improve the AD efficiency and allows an appropriate
33 process management (Carballa et al., 2015).

34 In recent years, an increasing body of literature has assessed the influence of
35 environmental selectors, like substrate type, ammonia concentration or temperature, in
36 the composition of AD microbiome (Regueiro et al., 2016; Vanwonterghem et al., 2015;
37 Zhang et al., 2014). Organic loading rate (OLR) is a critical AD operational parameter
38 that must be controlled to avoid disturbances in the process (Abendroth et al., 2015;
39 Rétfalvi et al., 2011). An OLR shock usually causes an imbalance between
40 hydrolysis/acidogenesis and methanogenesis steps. Consequently, volatile fatty acids
41 (VFA) accumulate, causing a pH drop and leading to methanogenesis failure (He et al.,
42 2017).

43 Under high VFA concentrations and low pH values, hydrogenotrophic methanogens,
44 that are more tolerant to stresses, dominate the metabolic pathways (Fotidis et al., 2014;
45 Goux et al., 2015). However, the behavior of bacterial communities during organic
46 overloading disturbances is more complex due to the high number of species and their
47 functional redundancy (Carballa et al., 2015; De Vrieze et al., 2013). Even when the
48 overloading is caused by the same co-substrate results of different studies are
49 contradictory. For example, Regueiro et al. (2015) used glycerol to induce OLR shocks
50 in pig-manure reactors observing the rise-up of *Bacteroidetes* and *Actinobacteria* phyla

51 and the overall decrease of *Firmicutes* despite the growth of *Tissierallaceae* family. In
52 contrast, in sewage sludge digesters under glycerol-induced OLR shocks, *Bacteroidetes*
53 decreased while *Firmicutes* increased due to the rise of *Veillonellaceae*;
54 *Ruminococcaceae* and *Clostridiales* Family X taxa (Ferguson et al. 2018; Braz et al.
55 2018; Ferguson et al. 2016). Similarly, the community response is not predictable by the
56 feedstock or the inoculum used in the reactors. For instance, in sewage sludge digesters
57 under overloadings induced with sugar beet pulp, *Bacteroidetes phylum* did not changed
58 in contrast with previous studies (Goux et al. 2015).

59 These conflicting results indicate that the knowledge about mechanisms controlling
60 changes in AD microbiome composition is still insufficient to predict the dynamics of
61 microbial community in AD process. Microbial community assembly processes might
62 include stochastic and deterministic mechanisms (Zhou et al., 2013, Ofiteru et al.,
63 2010). However, a growing body of literature indicates that deterministic processes,
64 particularly environmental selectors and species interactions, guide long-term
65 population changes in AD steady-state reactors (Peces et al. 2018; Ju et al. 2017; Lucas
66 et al. 2015; Vanwonterghem et al 2014; Fernández et al. 1999). During OLR shocks,
67 AD microbial community is affected by the external stressors (Ferguson et al. 2018; Xu
68 et al. 2018; Goux et al. 2015). Nevertheless, the importance of biotic interactions during
69 overloadings remains obscured as both synchronised and divergent changes in
70 composition has been observed (Ferguson et al. 2018; Braz. et al., 2018; Goux et al.
71 2015).

72 Co-occurrence networks can reveal the relationships between different microbial groups
73 in complex systems (Deng et al., 2012; Faust et al., 2012), but only few studies have
74 applied them to disentangle microbial interactions in AD. Xu et al. 2018, used this
75 analysis to find the connections between microorganisms and operational parameters

76 during and organic overloading event in anaerobic digesters, observing that the
77 *Firmicutes* phyla was the group most connected with biogas production. Rui et al.
78 (2015) investigated the microbiome of 43 anaerobic reactors using co-occurrence
79 networks finding that, despite high variations among microbial communities, the AD
80 core-community is organized into functional groups of microorganisms.

81 Understanding the mechanisms that govern the microbial species interactions during
82 AD imbalance events is needed to develop adequate process management strategies and
83 to avoid process failure (Widder et al., 2016). The importance of microbial interactions
84 in AD and other microbial systems during perturbations, has long being acknowledged
85 (Koch et al. 2013; Fernández et al. 1999) but remains scarcely explored. Therefore, this
86 study aimed to investigate the biotic interactions and dynamics that are established
87 during an OLR shock in sewage sludge digesters microbiomes in a thorough temporal
88 scale. To achieve this goal, the microbial communities of two parallel anaerobic
89 digesters feed on sewage sludge and operated identically, were exhaustively studied
90 with high-throughput amplicon sequencing during steady-state and acidosis induced
91 with glycerol as co-substrate.

92

93 **2. Materials and methods**

94 *2.1. Anaerobic reactors and experimental periods*

95 Two identical (R1 and R2) anaerobic continuous stirred (160 rpm, Heidolph
96 RZR 2041) tank reactors with a working volume of 14 L were operated in mesophilic
97 range (37°C) at a hydraulic retention time (HRT) of 20 days. They were inoculated
98 with approximately 14.0 g VSS/L (14.5 g VS/L) of anaerobic sludge from a full-scale
99 sewage sludge mesophilic anaerobic digester. The reactor feeding was prepared every
100 other week mixing primary and secondary sludge (70:30, v/v) and kept at 4 °C until

101 needed. During stabilization period (day 0 to 94), both reactors were operated at an
102 OLR of 1.8 g COD/ L d. Then, two periods were defined to evaluate the effect of
103 organic overloading on the AD microbiome: pre-shock (period 1) and shock (period 2).
104 During period 1 (day 95 to 102), the reactor biomass was sampled twice a day (at 10
105 and 16 h) to determine the microbiome fluctuation inherent to steady-state operation.
106 On day 102, the OLR was increased to 5 g COD/L d by adding glycerol waste, a residue
107 from a biodiesel production plant, and it was maintained until the end of the experiment
108 (day 105). The glycerol waste was selected based in its substantial worldwide
109 production (more than two million tons per year) and because it improves the
110 methanization efficiency, making it a great co-substrate for AD process (Ciriminna et al.
111 2014; Regueiro et al. 2012). The characterization of feedstock used during stabilization,
112 period 1 and 2 are shown in table 1. During this period (day 102 to 105), the AD
113 microbiome was examined by an intensive sampling scheme, namely biomass was
114 sampled 2-4 times per day (at 10, 13, 16 and 19 h). The detailed sampling scheme is
115 presented in Table A1 (supplementary information). Biomass samples consisted of well-
116 homogenized 2 mL triplicate aliquots that were stored at -80°C until the DNA
117 extraction. Additionally, biogas production was measured online; pH, VFAs, total (TA)
118 and partial (PA) alkalinity and total chemical oxygen demand (COD_t) were measured
119 each time that biomass samples were collected; and biogas composition was measured
120 once a day.

121

122 2.2. Analytical methods

123 Biogas production was measured with gas flow meter (μ flow - Bioprocess
124 control) and its composition was analyzed by gas chromatography (HP5890 Series II,
125 thermal conductivity detector, stainless steel column and helium as carrier gas) (García-

126 Gen et al., 2015). Physico-chemical parameters, such as pH, COD_t, total solids (TS),
127 volatile solids (VS), TA and PA were measured according to standard methods (APHA,
128 2012). VFA concentrations were determined by gas chromatography using a Hewlett
129 Packard 5890A device equipped with a flame ionization detector (García-Gen et al.,
130 2015). Reactor performance was compared between duplicates using a T-test,
131 considering p-value ≤ 0.01 , in IMB® SPSS® Statistics Version 22.

132

133 2.3. DNA extraction and sequence processing

134 Biomass samples were thawed and homogenized thoroughly in a vortex. For
135 each sample, DNA was extracted from 1 mL biomass for which the supernatant was
136 removed after 3 min of centrifugation at 20 000 g using the Stool DNA Isolation Kit
137 (Norgen, Thorold, Canada) according to manufacturer instructions. Total DNA
138 concentrations were quantified in a Qubit fluorometer (Thermo Fisher Scientific,
139 Waltham, MA, USA) and checked for size integrity by standard electrophoresis.
140 Fragments of the 16S rRNA gene were amplified for both *Bacteria* and *Archaea*
141 domains with primers including Illumina adaptors and barcodes. The V3V4 region of
142 the bacterial 16S rRNA gene was amplified with the primer pair S-D-Bact-0341-b-S-17
143 and S-D-Bact-0785-a-A (Klindworth et al. 2013). For *Archaea*, the V2V3 region was
144 amplified with the primer set Arch1F and Arch1R (Cruaud et al., 2014). An initial
145 polymerase chain reaction (PCR) was carried out with 3 ng of extracted DNA, 100 nM
146 for bacterial primers or 200 nM for archaeal primers and 1X Q5® High Fidelity Master
147 Mix (New England BioLabs) which contains the Q5® High Fidelity DNA polymerase,
148 2mM MgCl₂ and 200 μ M dNTPs. The PCR was performed as follows: an initial
149 denaturation at 98 °C for 30 s, followed by 20 or 22 cycles for *Bacteria* and *Archaea*
150 primers respectively that consisted on denaturation (98 °C) for 10 s, annealing for 20 s

151 and extension (72 °C) for 20 s; finishing with a final extension step at 72 °C during 2
152 min. The annealing temperature was 50 and 48 °C for bacterial and archaeal primers
153 respectively. These PCRs were followed by a second PCR to add the Illumina adapters
154 and barcodes to the amplicons that was run under similar conditions but only for 15
155 cycles and with an annealing temperature of 60 °C. Once constructed, DNA libraries
156 were checked for size and concentration using a Bioanalyzer (Bioanalyzer, Agilent
157 Technologies, Santa Clara, CA, USA). After library preparation, samples were
158 quantified by qPCR, pooled and sequenced in a MiSeq (Unidad de Genómica, Parque
159 Científico de Madrid). Paired-end reads (2 × 300) were generated according to the
160 manufacturer instructions (Illumina, Inc.).

161 The obtained reads were de-multiplexed and trimmed to remove Illumina
162 adapters, barcodes and sequencing primers. Then, paired reads were merged as
163 previously described (Eren et al., 2013) removing any read containing bases with a
164 quality score under 30, and using a minimum overlapping length 50 basepairs. Any
165 sequence with indeterminations was also removed from the analysis. Quality-filtered
166 sequences were analyzed for chimeras with VSEARCH (Rognes et al., 2016). After
167 quality filtering, 3.1 million bacterial and 1.4 million archaeal sequences were clustered
168 into 23,703 and 711 different OTUs, respectively (Table A2) using an open-reference
169 approach into Operational Taxonomic Units (OTU) at a 97% cutoff for sequence
170 similarity in the QIIME pipeline v.1.9.1 (Caporaso et al., 2010). The taxonomic
171 affiliations of OTUs were determined using the RDP classifier (Wang et al., 2007)
172 against the SILVA v123 database (Quast et al., 2013).

173

174 *2.4. Diversity and network analysis*

175 Richness and evenness indices were used to measure the within-sample bacterial
176 and archaeal community diversity due to organic overloading. Community richness was
177 estimated as the number of distinct OTUs, while community evenness, that measures
178 the equitability between the different species present in a community, was determined
179 as the Simpson evenness (E) index. Differences in community structure were assessed
180 using the Bray-Cutis dissimilarities. This index was used to determine the community
181 turnover through time of each reactor using a fixed window analysis to assess the
182 degree of community change every three days (Read et al. 2011). For this analysis, we
183 calculated the community structure change between the beginning and end of a period
184 of time as the Bray-Curtis dissimilarity within the same reactor. To make possible the
185 comparison of community turnover between the two experimental periods, period 1 was
186 subdivided into windows of the same temporal length than period 2 (3 consecutive
187 days). For period 2 dissimilarities were calculated between the initial and last day (from
188 102 to 105 days). Also, differences in community structure were visualized by
189 transformed-based Principal Component Analysis (tbPCA) after applying Hellinger
190 standardization to community data. Then community structure relationship with
191 operational parameters was analyzed by calculating the multiple regression of the
192 environmental variables with the ordination axes and the significance tested by a
193 permutation test. Next, significantly correlated ($p\text{-value} \leq 0.01$) operational parameters
194 were projected onto the ordination. These analyses were performed using the R
195 statistical environment with the Vegan package (Oksanen et al., 2016).

196 To find potential associations among microorganisms, a co-occurrence network
197 analysis was performed based on the abundant taxonomic groups at genus level.
198 Microbial networks were constructed with CoNet v.1.1.1. (Faust et al., 2012). Prior to
199 analysis, OTUs were grouped by taxonomy affiliations at genus level, and then the 323

200 genera with relative abundances over 0.1% in any of the samples were included in the
201 analysis. Compositional effects were avoided using bootstrap-renormalization
202 procedure (Faust et al., 2012). Two correlations (Spearman and Pearson) and two
203 distances (Bray Curtis and Kullback-Libler dissimilarities) were used to infer
204 relationships (edges) between microorganisms (nodes), discarding any linkage not
205 supported by at least two measurements. Benjamini-Hochberg procedure was used to
206 correct for multiple comparisons, discarding edges over the threshold of $q \leq 0.05$.
207 Resulting network was then analyzed to detect highly interacting groups of nodes
208 (clusters) using GLay algorithm (Su et al., 2010).

209

210 **3. Results and discussion**

211 *3.1. Rapid change of operational parameters to organic overloading*

212 Two replicate anaerobic reactors were seeded with the same inoculum and
213 operated for 105 days, that were divided into three operational periods: stabilization
214 period (day 0 to 94), pre-shock phase or period 1 (95-102 d) and overloading phase or
215 period 2 (102-105 d). All measured operational parameters were statistically similar in
216 both reactors throughout their operation (p -value ≤ 0.01). In stabilization period, the
217 CH_4 production was 0.9 g COD/L d, resulting in a methanization efficiency of around
218 45% during a very stable operation (Table 2). The same steady trend was observed for
219 pH, TA, PA and VFAs values that did not vary over the stabilization period. Likewise,
220 in period 1, reactors performance remained constant and comparable to the stabilization
221 period (Fig. 1). These results are similar to previous data in sewage sludge anaerobic
222 digestion literature (Razaviarani and Buchanan, 2014; Rétfalvi et al., 2011).

223 During OLR shock (period 2), the operational parameters showed three different
224 phases (Fig. 1). First, in the initial 9h of overloading, no significant changes were

225 observed in reactors functioning, except for the methanization efficiency, which
226 dropped to 22%. Second, between 9 and 33 h large changes were observed when the
227 VFA concentration rose to 2.4 g/L, and consequently, pH and alkalinities decreased.
228 Biogas composition changed from 61% to 30% CH₄ and from 30% to 60% CO₂ (Fig.
229 1A) in response to a pH decrease and consumption of PA (Fig. 1B). Finally, after 33 h
230 of overloading to the end of the experiment (72 h); the TA, PA and total VFA
231 concentrations stabilized (VFAs > 5 g/L) while the CH₄ fraction in the biogas increased
232 to 42% (48h), probably due to the decline of CO₂ production. The experiment was
233 stopped after 72 h of OLR shock, when pH was below 6 and CH₄ production decreased
234 to 0.49 COD/L d. Regardless the changes in some operational parameters, the TS and
235 VS remained stable during all experiment period.

236 Although butyric, acetic and valeric acids also accumulated, propionic acid had
237 the highest concentration among VFAs (Fig. 1C) as previously observed by authors that
238 used glycerol to induce the organic overloading (Ferguson et al., 2016; Regueiro et al.,
239 2015; Rétfalvi et al., 2011). However, the observed shifts of operational parameters in
240 these studies occurred later (after 2 to 5 days of overloading) than in study (only 24h).
241 Differences in reactor operation could explain this observation, like more TA available
242 or prior acclimatization of the community to glycerol as co-substrate.

243

244 3.2. Microbial community diversity and structure reflected the OLR shock

245 The OLR shock decreased archaeal but not bacterial richness. It also affected the
246 uniformity of both communities although in an opposite trend: *Bacteria* became more
247 uneven, while *Archaea* became more even (Fig 2). A reduction on microbial diversity
248 has been observed in other studies of OLR shocks in anaerobic reactors (Fitamo et al.,
249 2017; Kampmann et al., 2014; Xu et al., 2018). It has been proposed that the increase of

250 VFAs induced by the OLR shock inhibits the growth of some microorganisms (Fitamo
251 et al., 2017). In this sense, our results suggest that while several *Bacteria* become
252 inhibited resulting in the dominance of less organisms, some *Archaea* might perish
253 under period 2 conditions causing a loss of species.

254 Community structure was also modified during the organic overloading
255 following similar changing trends in both R1 and R2 that were correlated with the
256 increase of OLR, VFAs accumulation and the decrease of pH (p-value ≤ 0.01 ; Fig 3); in
257 concordance with other observations of structure shift during overloading influenced by
258 those operational parameters (Goux et al., 2015; Hori et al., 2006; Xu et al., 2018).

259 In addition, community structure was different between R1 and R2 even though
260 they were inoculated from the same source. Communities with diverging taxonomic
261 compositions under stable environments have been repeatedly observed in bioreactors
262 and other environments (Fernandez-Gonzalez et al., 2016; Louca et al., 2018) which can
263 be the result of stochastic immigration and ecological drift (Zhou and Ning, 2017);
264 although, as recently discussed by Louca et al. (2018), taxonomic turnover is generally
265 not explained by ecological drift and can be driven by intrinsic, mostly biological,
266 deterministic processes.

267 The temporal change of the AD microbiome or community turnover, became
268 accelerated during overloading. In period 1, community turnover were 19 ± 2 and $8\pm 4\%$
269 for *Bacteria* and *Archaea* respectively, likewise to other observations on bioreactors
270 during steady-state periods (Hai et al., 2014). In contrast, during period 2 microbial
271 community turnover largely increased (*Bacteria*: $48\pm 2\%$ and *Archaea* $39\pm 1\%$)
272 indicating the strong influence of the sudden OLR shock provoked by the addition of
273 glycerol as a new co-substrate on the microbial community organization and its low
274 resistance to change in face of a perturbation. Microbial communities of wastewater

275 treatment systems can have short reaction times toward sudden external perturbations
276 (Braz et al. 2018; Koch et al. 2013). In other studies, when the microbial community
277 was gradually adapted to a new co-substrate, for example, by applying a gradual OLR
278 increase or pulse feeding; the AD microbiome structure was more resistant to organic
279 overloading or other process imbalances (Ferguson et al. 2016; De Vrieze et al. 2013;
280 Ghasimi et al. 2015).

281

282 *3.3. Organic overloading changed community composition and induced a temporal*
283 *succession of co-occurring microorganisms.*

284 Both *Bacteria* and *Archaea* community compositions were similar between
285 replicated reactors despite the differences in community structure (Fig. 4). Community
286 composition was quite stable in period 1, when over 70% of *Bacteria* belonged to phyla
287 *Bacteroidetes*, *Firmicutes*, *Proteobacteria* and *Chloroflexi* (Fig. A1) and the most
288 abundant genera were *Sedimentibacter* sp. and two unknown *Bacteroidales* taxa (Fig
289 4A, Fig. A1). Most *Archaea* taxa were methanogens, dominated by *Methanosaeta* sp.
290 and an unknown *Methanomicrobial* genus (Fig. 4B, Fig. A1). These groups of
291 organisms are commonly found in sewage sludge anaerobic digesters and many have
292 been described as part of the core community of full-scale mesophilic sludge digesters
293 (Mei et al., 2017).

294 In period 2, community composition was altered and a temporal succession of
295 the dominant microorganisms occurred (Fig 4). The changes included initial increments
296 of *Veillonellaceae* and *Treponema* bacterial groups as well as *Methanosaeta* and
297 *Methanoculleus* methanogenic genera; microorganisms that decreased towards the end
298 of the experiment. It is widely known that AD microbial community composition is
299 commonly affected by organic overloading (Goux et al., 2015; Regueiro et al., 2015).

300 AD process is possible due to the activity of several microorganisms that form a
301 highly-interconnected community in which several species establish different types of
302 biological associations, such as mutualism, symbiosis or competence. The temporal
303 succession of organisms and their potential associations during the organic overloading
304 was explored by a network analysis on the dominant fraction of the microbial
305 community (relative abundances > 0.1% in any of the samples). Nine highly
306 interconnected groups or clusters of co-occurring microorganisms could be identified
307 (Fig 5, Fig A2), that altogether contained 63.7 ± 6.9 and 95.5 ± 1.9 % of the bacterial
308 and archaeal communities, respectively. These clusters were characterized by distinct
309 temporal trends, indicating the occurrence of a temporal succession of related groups of
310 microorganisms during the OLR shock (Fig. 6, Fig. A3). Clusters also had different
311 taxonomic compositions (Fig. 7, Table A3). While clusters 2, 4, 6 and 7 contained both
312 archaeal and bacterial taxa; clusters 1, 3, 5, 8 and 9 were solely composed by *Bacteria*.
313 Only abundant clusters (total accumulated relative abundance by domain > 5% on any
314 sample, Fig. 6) are further discussed.

315 During the first 9 hours of overloading and before operational variables showed
316 relevant shifts, the relative abundances of several clusters changed respect to the
317 baseline observed during period 1. While clusters 3 (only *Bacteria*) and 7 increased,
318 clusters 4, 5, 6 and 9 decreased (Fig. 6); trends that overall, were maintained during the
319 increment of propionate concentration between 9 and 48 h of overloading (Fig. 1). The
320 most abundant organisms in cluster 3 were unknown members of *Veillonellaceae*
321 family (Fig 7, Table A3), that is a group of fermentative organisms commonly detected
322 in anaerobic environments rich in organic matter (Marchandin and Jumas-Bilak, 2014),
323 which

324 reached a maximum value of 21.9 % of bacteria relative abundance. In these reactors,
325 this group likely drove the glycerol fermentation into propionate, a process described
326 for many genera of this family such as *Anaerosinus* (Strömpl et al., 1999). The second
327 most abundant organisms in cluster 3 was *Cloacamonaceae* uncultured genus W22,
328 which is the main responsible for the rise of *Candidatus* Cloacimonetes (WWE1)
329 phylum observed during period 2 (Fig. A1.A). The increment of *Candidatus*
330 Cloacimonetes (WWE1) have been already reported during OLR shocks in anaerobic
331 digesters related to the accumulation of propionate as these organisms might ferment
332 aminoacids and syntrophically oxidize propionate into H₂, CO₂ and acetate (Goux et al.,
333 2015; Hagen et al., 2014; Pelletier et al., 2008). Therefore, the increase of the
334 uncultured W22 genera is likely linked to the production of propionate by
335 *Veillonellaceae*, suggesting a commensal relationship between both organisms. Many
336 other organisms of cluster 3 belonged to *Spirochaetes* phylum that might be able to
337 perform syntrophic acetate oxidation (Lee et al., 2013).

338 In *Bacteria*, cluster 3 displaced microorganisms mostly from clusters 4, 6 and 9,
339 which are rich in different types of hydrolytic and fermentative bacteria. Cluster 4, that
340 was the dominant bacterial group in period 1, was mostly composed by an unknown
341 *Bacteoidales* family SB-1 (Fig 7, Table A3). *Bacteroidales* is a broad order containing
342 mainly anaerobic saccharolytic organisms, although other substrates might be used as
343 well (Krieg et al., 2010). Other groups found within cluster 4 were also hydrolytic or
344 fermentative bacteria like *Ruminococcaceae*, *Anaerolinaceae* T78 and *Synergistaceae*
345 vadinCA02 group, from *Synergistetes* phylum, that exhibits obligatory anaerobic
346 aminolytic metabolism. Cluster 9 was also dominated by fermenters, mainly
347 *Sedimentibacter*, that only ferments pyruvate and amino acids, accompanied by other
348 fermentative *Firmicutes* like *Anaerovorax* (Fig 7, Table A3). Most syntrophic bacteria

349 (i.e.: *Syntrophomonas* or *Syntrophus*, Fig 7, Table A3) located in Cluster 6, also
350 diminished in abundance during the overloading. The latter can be related to the high
351 propionate concentrations, which quickly reached values over 2 g/L (24h) and can
352 inhibits syntrophic bacteria (Ban Q et al., 2013).

353 Archaeal cluster 7 also incremented during the initial 48 hours of overloading,
354 displacing archaea within clusters 4 and 6 which only contains hydrogenotrophic
355 methanogens (Fig 7, Table A3). Cluster 7 contained the largest archaeal diversity, with
356 9 taxa, representing on average the 58.3 ± 15.7 % of archaeal community. The principal
357 organisms in the cluster was *Methanosaeta* (up to 68.5 % of Archaea), which was
358 accompanied by *Methanoculleus*, *Methanobrevibacter* or *Methanobacterium*, all
359 hydrogenotrophic methanogens. *Methanosaeta* became the most dominant methanogen
360 during most of the overloading period. It is a well-known acetoclastic methanogen that
361 grows in low levels of acetate. It has been suggested that *Methanosaeta* could survive
362 only in low VFA concentrations (Griffin et al., 1998). However, our data showed that
363 *Methanosaeta* can temporally withstand VFAs concentrations of mostly propionic acid,
364 between 2.5 – 5.0 g/L. Franke-Whittle et al. (2014) also reported a single observation of
365 an AD reactor with high VFA concentration (3.9 g/L of propionate and 1.25 g/L of
366 acetate) dominated by *Methanosaeta*. These data suggest that the shift between
367 hydrogenotrophic (*Methanoculleus* sp.) and aceticlastic (*Methanosaeta* sp.)
368 methanogens as a warning indicator of acidosis during high OLR (Goux et al., 2015) is
369 not universal.

370 After 48h of overloading, trends of the most dominant clusters changed. By then,
371 more than 5.5 g/L of VFAs, mostly propionic and butyric acids, were already
372 accumulated, lowering the pH (6.2) in the reactors. pH decreased even further after 72 h
373 (5.8), when valeric acid concentrations also increased. In parallel, a succession between

374 different types of fermentative bacteria was observed. After 48h of overload,
375 *Veillonellaceae* and its cohort (cluster 3) become replaced by *Bacteroidales* and
376 *Synergistetes* of cluster 4, including a transitional increment of *Porphyromonadaceae*
377 (cluster 5) at 54 h and increment of *Chitinophagaceae* (cluster 2) at the end of the
378 experiment (Fig. 7, Table A3). Simultaneously, *Methanosaeta* (cluster 7) drastically
379 dropped in abundance to finally be replaced by the putative hydrogenotrophic
380 methanogen, *Methanobacteriales_WSA2* (cluster 2, Fig. 7, Table A3); although the
381 methane production strongly decreased.

382 The intense timeframe of this study allowed to partially unveil fast-changing
383 biotic interactions in the AD microbiome. Acidogenic bacteria are known to react
384 immediately when exposed to high substrate amounts by increasing their metabolic
385 activity and cell numbers (Schnürer et al. 1999). The acidogenic that reacted faster and
386 more intensely to the OLR shock was *Veillonellaceae* family. The rise of this taxon
387 during glycerol OLR shocks seems to be common (Braz et al. 2018; Ferguson et al.
388 2018), probably due to its ability to degrade glycerol, but it is not universal (Regueiro et
389 al. 2015). Similarly, a succession of microorganisms seems to be a common feature
390 after an OLR shock, but the specific populations that are involved in the temporal
391 succession are far from common among AD digesters, even in the case of using the
392 same type feedstock or co-substrate (Braz et al 2018; Fitamo et al 2017; Goux et al.
393 2015; Regueiro et al. 2015).

394 Functional redundancy has been proven in long-term AD reactors (Theuerl et al
395 2015) and it is known that other microorganisms can overtake missing functions during
396 perturbations (Fernández et al. 1999). The observed temporal succession among
397 different taxa of the same functional groups (i.e.: fermenters, methanogens) during the
398 changing conditions of the overloading event is a strong indication of the importance of

399 temporal metabolic niche effects (mechanisms selecting organisms able to exploit
400 specific metabolic pathways, Louca et al. 2018) in AD microbiome under OLR shocks.
401 In these events, several factors are selecting between functionally redundant
402 microorganisms. The introduction of a new substrate, the availability of its products of
403 degradation that promotes commensalism relationships, the changing pH conditions and
404 other biotic interactions like competition, are mechanisms creating new niches. Co-
405 occurring microorganisms likely established positive biological interactions, that in
406 some cases could be inferred (i.e. cluster 3). In other cases, co-occurring organisms are
407 limited by similar factors (i.e. cluster 6). However, the lack of taxonomic resolution and
408 the large fraction of microbial diversity still undescribed obscure the detailed nature of
409 the biotic interactions. As our knowledge about uncultured species and their capabilities
410 advances, we would be able to uncover the detailed nature of the biological processes.

411

412 **4. Conclusion**

413 The effect of a sudden increase of OLR by the addition of glycerol as a co-
414 substrate affected AD process performance similarly in both replicated reactors,
415 producing a fast VFA accumulation, reactor acidification and final AD process failure.
416 The overloading induced a redistribution in the equitability of microorganisms and a
417 loss of *Archaea* species, but also an increment in community temporal turnover,
418 indicating the lack of resilience of these microbiomes that were not previously exposed
419 to the added co-substrate. AD microbiome turnover seems to be driven by community
420 internal dynamics during steady-state AD operation whereas, an OLR shock imposes
421 environmental selecting criteria. The changing environment during overloading caused
422 a temporal succession of functionally redundant microorganisms suggesting niche
423 specialization. Several mutualistic and competitive relationships among groups of

424 microorganisms occurred, although most of the details of those mechanisms remain
425 obscured due to the lack of information about genetic and physiological capabilities of
426 many microbial clades of AD microbiome. Increments in VFAs are not always adverse
427 for *Methanosaeta*, and reactor acidosis can occur, at least transitorily, without a decline
428 of this methanogen. Overall, the observed succession of functionally redundant
429 microorganisms influenced by changes on environment and species interrelationships
430 highlights that deterministic processes drive AD community dynamics during OLR
431 shocks.

432

433 **Conflicts of interest**

434 None

435

436 **Acknowledgments**

437 This research was supported by the Spanish Government (AEI) through DCTI
438 (SmartGreenGas project, 2014-CE224). The authors belong to the Galician Competitive
439 Research Group GRC (ED431C 2017/29) and the Strategic Partnership for Research in
440 Environmental Technologies of the *Universidade de Santiago de Compostela*
441 (CRETUS, AGRUP2015/02). All these programs are co-funded by FEDER (UE).
442 GHRB PhD fellowship is supported by CAPES (BEX-2160/2015-03) Foundation,
443 Ministry of Education of Brazil, Brasília – DF 70040-020, Brazil. Computational
444 resources were kindly provided by the Galician Center of Supercomputation (CESGA).

445

446 **Appendix A. Supplementary information**

447 Supplementary data associated with this article can be found in the online version

448

449 **References**

- 450 Abendroth, C., Vilanova, C., Günther, T., Luschning, O., Porcar, M., 2015. *Eubacteria*
451 and *Archaea* communities in seven mesophile anaerobic digester plants in
452 Germany. *Biotechnol. Biofuels* 8, 87. <https://doi.org/10.1186/s13068-015-0271-6>
- 453 APHA, 2012. Standard methods for the examination of water and wastewater, 20th ed.
454 Washington, DC, USA.
- 455 Braz, G.H.R., Fernandez-Gonzalez, N., Lema, J.M., Carballa, M., 2018. The time
456 response of anaerobic digestion microbiome during an organic loading rate shock.
457 *Appl. Microbiol. Biotechnol.* doi: 10.1007/s00253-018-9383-9
- 458 Caporaso, J.G., Kuczynski, J., Stombaugh, J., Bittinger, K., Bushman, F.D., Costello,
459 E.K., Fierer, N., Peña, A.G., Goodrich, J.K., Gordon, J.I., Huttley, G.A., Kelley,
460 S.T., Knights, D., Koenig, J.E., Ley, R.E., Lozupone, C.A., Mcdonald, D.,
461 Muegge, B.D., Pirrung, M., Reeder, J., Sevinsky, J.R., Turnbaugh, P.J., Walters,
462 W.A., Widmann, J., Yatsunenko, T., Zaneveld, J., Knight, R., 2010. QIIME allows
463 analysis of high- throughput community sequencing data. *Nat. Methods* 7, 335–
464 336. <https://doi.org/10.1038/nmeth0510-335>
- 465 Carballa, M., Regueiro, L., Lema, J.M., 2015. Microbial management of anaerobic
466 digestion: Exploiting the microbiome-functionality nexus. *Curr. Opin. Biotechnol.*
467 33, 103–111. <https://doi.org/10.1016/j.copbio.2015.01.008>
- 468 Ciriminna, R., Pina, C. Della, Rossi, M., Pagliaro, M., 2014. Understanding the glycerol
469 market. *Eur. J. Lipid. Sci. Technol* 116:1432–1439. <https://doi.org/10.1002/ejlt.201400229>.
- 471 Cruaud, P., Vigneron, A., Lucchetti-Miganeh, C., Ciron, P.E., Godfroy, A., Cambon-
472 Bonavita, M.A., 2014. Influence of DNA extraction method, 16S rRNA targeted
473 hypervariable regions, and sample origin on microbial diversity detected by 454

- 474 pyrosequencing in marine chemosynthetic ecosystems. *Appl. Environ. Microbiol.*
475 80, 4626–4639. <https://doi.org/10.1128/AEM.00592-14>
- 476 De Vrieze, J., Verstraete, W., Boon, N., 2013. Repeated pulse feeding induces
477 functional stability in anaerobic digestion. *Microb. Biotechnol.* 6, 414–424.
478 <https://doi.org/10.1111/1751-7915.12025>
- 479 Deng, Y., Jiang, Y.-H., Yang, Y., He, Z., Luo, F., Zhou, J., 2012. Molecular ecological
480 network analyses. *BMC Bioinformatics* 13, 113. [https://doi.org/10.1186/1471-](https://doi.org/10.1186/1471-2105-13-113)
481 [2105-13-113](https://doi.org/10.1186/1471-2105-13-113)
- 482 Eren, A.M., Vineis, J.H., Morrison, H.G., Sogin, M.L., 2013. A Filtering method to
483 generate high quality short reads using Illumina paired-end technology. *PLoS One*
484 8, 6–11. <https://doi.org/10.1371/journal.pone.0066643>
- 485 Faust, K., Sathirapongsasuti, J.F., Izard, J., Segata, N., Gevers, D., Raes, J.,
486 Huttenhower, C., 2012. Microbial co-occurrence relationships in the human
487 microbiome. *PLoS Comput. Biol.* 8, e1002606.
488 <https://doi.org/10.1371/journal.pcbi.1002606>
- 489 Ferguson, R.M.W., Coulon, F., Villa, R., 2016. Organic loading rate: A promising
490 microbial management tool in anaerobic digestion. *Water Res.* 100, 348–356.
491 <https://doi.org/10.1016/j.watres.2016.05.009>
- 492 Ferguson, R.M.W., Coulon, F., Villa, R., 2018. Understanding microbial ecology can
493 help improve biogas production in AD. *Sci. Total Environ.* 642, 754-763.
494 <https://doi.org/10.1016/j.scitotenv.2018.06.007>
- 495 Fernandez-Gonzalez, N., Huber, J.A., Vallino, J.J., 2016. Microbial communities are
496 well adapted to disturbances in energy input. *mSystems* 1(5):e00117-16
497 <https://doi.org/10.1128/mSystems.00117-16>.
- 498 Fernández, A., Huang, S., Seston, S., Xing, J. Hickey, R., Criddle, C., Tiedje, J., 1999.

- 499 How stable is Stable? Function versus community composition. *Appl. Environ.*
500 *Microbiol.* 65, 3697-3704
- 501 Fitamo, T., Treu, L., Boldrin, A., Sartori, C., Angelidaki, I., Scheutz, C., 2017.
502 Microbial population dynamics in urban organic waste anaerobic co-digestion with
503 mixed sludge during a change in feedstock composition and different hydraulic
504 retention times. *Water Res.* 118, 261–271.
505 <https://doi.org/10.1016/j.watres.2017.04.012>
- 506 Fotidis, I.A., Karakashev, D., Angelidaki, I., 2014. The dominant acetate degradation
507 pathway/methanogenic composition in full-scale anaerobic digesters operating
508 under different ammonia levels. *Int. J. Environ. Sci. Technol.* 11, 2087–2094.
509 <https://doi.org/10.1007/s13762-013-0407-9>
- 510 Franke-Whittle, I.H., Walter, A., Ebner, C., Insam, H., 2014. Investigation into the
511 effect of high concentrations of volatile fatty acids in anaerobic digestion on
512 methanogenic communities. *Waste Manag.* 34, 2080–2089.
513 <https://doi.org/10.1016/j.wasman.2014.07.020>
- 514 García-Gen, S., Sousbie, P., Rangaraj, G., Lema, J.M., Rodríguez, J., Steyer, J.P.,
515 Torrijos, M., 2015. Kinetic modelling of anaerobic hydrolysis of solid wastes,
516 including disintegration processes. *Waste Manag.* 35, 96–104.
517 <https://doi.org/10.1016/j.wasman.2014.10.012>
- 518 Ghasimi, D.S.M., Tao, Y., De Kreuk, M., Zandvoort, M.H., Van Lier, J.B., 2015.
519 Microbial population dynamics during long-term sludge adaptation of thermophilic
520 and mesophilic sequencing batch digesters treating sewage fine sieved fraction at
521 varying organic loading rates. *Biotechnol. Biofuels* 8, 1–15.
522 <https://doi.org/10.1186/s13068-015-0355-3>
- 523 Goux, X., Calusinska, M., Lemaigre, S., Marynowska, M., Klocke, M., Udelhoven, T.,

- 524 Benizri, E., Delfosse, P., 2015. Microbial community dynamics in replicate
525 anaerobic digesters exposed sequentially to increasing organic loading rate,
526 acidosis, and process recovery. *Biotechnol. Biofuels* 8, 122.
527 <https://doi.org/10.1186/s13068-015-0309-9>
- 528 Griffin, M.E., McMahon, K.D., Mackie, R.I., Raskin, L., 1998. Methanogenic
529 population dynamics during start-up of anaerobic digesters. *Biotechnol. Bioeng.*
530 57, 346–355.
- 531 Hagen, L.H., Vivekanand, V., Linjordet, R., Pope, P.B., Eijsink, V.G.H., Horn, S.J.,
532 2014. Microbial community structure and dynamics during co-digestion of whey
533 permeate and cow manure in continuous stirred tank reactor systems. *Bioresour.*
534 *Technol.* 171, 350–359. <https://doi.org/10.1016/j.biortech.2014.08.095>
- 535 Hai, R., Wang, Y., Wang, X., Li, Y., Du, Z., 2014. Bacterial community dynamics and
536 taxa-time relationships within two activated sludge bioreactors. *PLoS One* 9, 1–8.
537 <https://doi.org/10.1371/journal.pone.0090175>
- 538 He, Q., Li, L., Peng, X., 2017. Early Warning Indicators and microbial mechanisms for
539 process failure due to organic overloading in food waste digesters. *J. Environ. Eng.*
540 143, 04017077. [https://doi.org/10.1061/\(ASCE\)EE.1943-7870.0001280](https://doi.org/10.1061/(ASCE)EE.1943-7870.0001280)
- 541 Hori, T., Haruta, S., Ueno, Y., Ishii, M., Igarashi, Y., 2006. Dynamic transition of a
542 methanogenic population in response to the concentration of volatile fatty acids in
543 a thermophilic anaerobic digester. *Appl. Environ. Microbiol.* 72, 1623–30.
544 <https://doi.org/10.1128/AEM.72.2.1623-1630.2006>
- 545 Ju, F., Lau, F., Zhang, T., 2017. Linking microbial community, environmental variables,
546 and methanogenesis in anaerobic biogas digesters of chemically enhanced primary
547 treatment sludge. *Environ. Sci. Technol.* 51, 3982-3992.
548 <https://doi.org/10.1021/acs.est.6b06344>

- 549 Kampmann, K., Ratering, S., Geißler-Plaum, R., Schmidt, M., Zerr, W., Schnell, S.,
550 2014. Changes of the microbial population structure in an overloaded fed-batch
551 biogas reactor digesting maize silage. *Bioresour. Technol.* 174, 108–117.
552 <https://doi.org/10.1016/j.biortech.2014.09.150>
- 553 Klindworth, A., Pruesse, E., Schweer, T., Peplies, J., Quast, C., Horn, M., Glöckner,
554 F.O., 2013. Evaluation of general 16S ribosomal RNA gene PCR primers for
555 classical and next-generation sequencing-based diversity studies. *Nucleic Acids*
556 *Res.* 41, 1–11. <https://doi.org/10.1093/nar/gks808>
- 557 Koch, C., Fetzer, I., Schmidt, T., Harms, H., Müller, S., 2013. Monitoring functions in
558 managed microbial systems by cytometric bar coding. *Environ. Sci. Technol.* 47,
559 1753-1760. <https://doi.org/10.1021/es3041048>
- 560 Krieg, N.R., Ludwig, W., Euzéby, J., William, B.W., 2010. Phylum XIV. *Bacteroidetes*
561 *phyl. nov.*, in: Krieg, N.R., Staley, J., Brown, D.R., Hedlund, B.P., Paster, B.J.,
562 Ward, N.L., Ludwig, W., Whitman, W.B. (Eds.), *Bergey's Manual of Systematic*
563 *Bacteriology-Volumen Four: The Bacteroidetes, Spirochaetes, Tenericutes*
564 *(Mollicutes), Acidobacteria, Fobrobacteres, Fusobacteria, Dictyoglomi,*
565 *Gemmatimonadetes, Lentisphaerae, Verrucomicrobia, Chlamydiae, and*
566 *Planctomycetes*. Springer, New York, Dordrecht, Heidelberg, London, pp. 25–104.
567 <https://doi.org/10.1007/978-0-387-68572-4>
- 568 Lee, S.H., Park, J.H., Kang, H.J., Lee, Y.H., Lee, T.J., Park, H.D., 2013. Distribution
569 and abundance of *Spirochaetes* in full-scale anaerobic digesters. *Bioresour.*
570 *Technol.* 145, 25–32. <https://doi.org/10.1016/j.biortech.2013.02.070>
- 571 Louca, S., Polz, M.F., Mazel, F., Albright, M.B.N., Huber, J.A., O'Connor, M.I.,
572 Ackermann, M., Hahn, A.S., Srivastava, D.S., Crowe, S.A., Doebeli, M., Parfrey,
573 L.W., 2018. Function and functional redundancy in microbial systems. *Nat. Ecol.*

- 574 Evol. <https://doi.org/10.1038/s41559-018-0519-1>
- 575 Lucas, R., Kuchenbuch, A., Fetzter, I., Harms, H., Kleinstaubler, S., 2015. Long-term
576 monitoring reveals stable and remarkably similar microbial communities in parallel
577 full-scale biogas reactors digesting energy crops. *FEMS Microbiol Eco.* 91, fiv004.
578 <https://doi.org/10.1093/femsec/fiv004>
- 579 Marchandin, H., Jumas-Bilak, E., 2014. The family *Veillonellaceae*, in: Rosenberg, E.,
580 Delong, E.F., Lory, S., Stackebrandt, E., Thompson, F. (Eds.), *The Prokaryotes:*
581 *Firmicutes and Tenericutes*. Springer-Verlag, Berlin, Heidelberg, pp. 433–453.
582 <https://doi.org/10.1007/978-3-642-30120-9>
- 583 Mei, R., Nobu, M.K., Narihiro, T., Kuroda, K., Muñoz Sierra, J., Wu, Z., Ye, L., Lee,
584 P.K.H., Lee, P.-H., van Lier, J.B., McInerney, M.J., Kamagata, Y., Liu, W.-T.,
585 2017. Operation-driven heterogeneity and overlooked feed-associated populations
586 in global anaerobic digester microbiome. *Water Res.* 124, 77–84.
587 <https://doi.org/10.1016/j.watres.2017.07.050>
- 588 Ofiteru, I.D., Lunn, M., Curtis, T.P., Wells, G.F., Criddle, C.S., Francis, C. a, Sloan,
589 W.T., 2010. Combined niche and neutral effects in a microbial wastewater
590 treatment community. *Proc. Natl. Acad. Sci. U. S. A.* 107, 15345–15350.
591 <https://doi.org/10.1073/pnas.1000604107>
- 592 Oksanen, J., Blanchet, F.G., Friendly, M., Kindt, R., Legendre, P., McGlenn, D.,
593 Minchin, P.R., O'Hara, R.B., Simpson, G.L., Solymos, P., Stevens, M.H.H.,
594 Szoecs, E., Wagner, H., 2016. vegan: Community Ecology Package. R package
595 version 2.4-1.
- 596 Pelletier, E., Kreimeyer, A., Bocs, S., Rouy, Z., Gyapay, G., Chouari, R., Rivière, D.,
597 Ganesan, A., Daegelen, P., Sghir, A., Cohen, G.N., Médigue, C., Weissenbach, J.,
598 Le Paslier, D., 2008. “*Candidatus Cloacamonas acidaminovorans*”: Genome

- 599 sequence reconstruction provides a first glimpse of a new bacterial division. *J.*
600 *Bacteriol.* 190, 2572–2579. <https://doi.org/10.1128/JB.01248-07>
- 601 Peces, M., Astals, S., Jensen, P.D., Clarke, W.P., 2018. Deterministic mechanisms
602 define the long-term anaerobic digestion microbiome and its functionality
603 regardless of the initial microbial community. *Water Res.* 141, 366–376.
604 <https://doi.org/10.1016/j.watres.2018.05.028>
- 605 Quast, C., Pruesse, E., Yilmaz, P., Gerken, J., Schweer, T., Yarza, P., Peplies, J.,
606 Glöckner, F.O., 2013. The SILVA ribosomal RNA gene database project:
607 improved data processing and web-based tools. *Nucleic Acids Res.* 41, D590–
608 D596. <https://doi.org/10.1093/nar/gks1219>
- 609 Razaviarani, V., Buchanan, I.D., 2014. Reactor performance and microbial community
610 dynamics during anaerobic co-digestion of municipal wastewater sludge with
611 restaurant grease waste at steady state and overloading stages. *Bioresour. Technol.*
612 172, 232–240. <https://doi.org/10.1016/j.biortech.2014.09.046>
- 613 Read, S., Marzorati, M., Guimares, B.C.M., Boon, N., 2011. Microbial resource
614 management revisited: successful parameters and new concepts. *Appl. Microbiol.*
615 *Biotechnol.* 90, 861–871. <https://doi.org/10.1007/s00253-011-3223-5>
- 616 Regueiro, L., Carballa, M., Álvarez, J.A., Lema, J.M., 2012. Enhanced methane
617 production from pig manure anaerobic digestion using fish and biodiesel wastes as
618 co-substrates. *Bioresour. Technol.* 123, 507–513.
619 <https://doi.org/10.1016/j.biortech.2012.07.109>
- 620 Regueiro, L., Carballa, M., Lema, J.M., 2016. Microbiome response to controlled shifts
621 in ammonium and LCFA levels in co-digestion systems. *J. Biotechnol.* 220, 35–44.
622 <https://doi.org/10.1016/j.jbiotec.2016.01.006>
- 623 Regueiro, L., Lema, J.M., Carballa, M., 2015. Key microbial communities steering the

- 624 functioning of anaerobic digesters during hydraulic and organic overloading
625 shocks. *Bioresour. Technol.* 197, 208–216.
626 <https://doi.org/10.1016/j.biortech.2015.08.076>
- 627 Rétfalvi, T., Tukacs-Hájos, A., Albert, L., Marosvölgyi, B., 2011. Laboratory scale
628 examination of the effects of overloading on the anaerobic digestion by glycerol.
629 *Bioresour. Technol.* 102, 5270–5275.
630 <https://doi.org/10.1016/j.biortech.2011.02.020>
- 631 Rognes, T., Flouri, T., Nichols, B., Quince, C., Mahé, F., 2016. VSEARCH: a versatile
632 open source tool for metagenomics. *PeerJ* 4, e2584.
633 <https://doi.org/10.7717/peerj.2584>
- 634 Rui, J., Li, J., Zhang, S., Yan, X., Wang, Y., Li, X., 2015. The core populations and co-
635 occurrence patterns of prokaryotic communities in household biogas digesters.
636 *Biotechnol. Biofuels* 8, 1–15. <https://doi.org/10.1186/s13068-015-0339-3>
- 637 Schnürer, A., Sellner, G., Svensson, B. H., 1999. Mesophilic syntrophic acetate
638 oxidation during methane formation in biogas reactors. *FEMS Microbiol. Ecol.* 29,
639 249-261.
- 640 Strömpl, C., Tindall, B.J., Jarvis, G.N., Lünsdorf, H., Moore, E.R., Hippe, H., 1999. A
641 re-evaluation of the taxonomy of the genus *Anaerovibrio*, with the reclassification
642 of *Anaerovibrio glycerini* as *Anaerosinus glycerini* gen. nov., comb. nov., and
643 *Anaerovibrio burkinabensis* as *Anaeroarcus burkinensis* [corrig.] gen. nov., comb.
644 nov. *Int. J. Syst. Bacteriol.* 49, 1861–1872. [https://doi.org/10.1099/00207713-49-4-](https://doi.org/10.1099/00207713-49-4-1861)
645 1861
- 646 Su, G., Kuchinsky, A., Morris, J.H., States, D.J., Meng, F., 2010. GLay: Community
647 structure analysis of biological networks. *Bioinformatics* 26, 3135–3137.
648 <https://doi.org/10.1093/bioinformatics/btq596>

- 649 Theuerl, S. Kohrs, F., Benndorf, D., Maus, I., Wibberg, D., Schlüter, A., Kausmann, R.,
650 Heiermann, M., Rapp, E., Reichl, U., Pühler, A., Klocke, M., 2015. Community
651 shifts in a well-operating agricultural biogas plant: how process variations are
652 handled by the microbiome. *Appl. Microbiol. Biotechnol.* 99, 7791-7803.
653 <https://doi.org/10.1007/s00253-015-6627-9>
- 654 Vanwonterghem, I., Jensen, P.D., Dennis, P.G., Hugenholtz, P., Rabaey, K., Tyson,
655 G.W., 2014. Deterministic processes guide long-term synchronised population
656 dynamics in replicate anaerobic digesters. *ISME J.* 8, 2015–2028.
657 <https://doi.org/10.1038/ismej.2014.50>
- 658 Vanwonterghem, I., Jensen, P.D., Rabaey, K., Tyson, G.W., 2015. Temperature and
659 solids retention time control microbial population dynamics and volatile fatty acid
660 production in replicated anaerobic digesters. *Sci. Rep.* 5, 1–8.
661 <https://doi.org/10.1038/srep08496>
- 662 Wang, Q., Garrity, G.M., Tiedje, J.M., Cole, J.R., 2007. Naive Bayesian classifier for
663 rapid assignment of rRNA sequences into the new bacterial taxonomy. *Appl.*
664 *Environ. Microbiol.* 73, 5261–7. <https://doi.org/10.1128/AEM.00062-07>
- 665 Widder, S., Allen, R.J., Pfeiffer, T., Curtis, T.P., Wiuf, C., Sloan, W.T., Cordero, O.X.,
666 Brown, S.P., Momeni, B., Shou, W., Kettle, H., Flint, H.J., Haas, A.F., Laroche,
667 B., Kreft, J., Rainey, P.B., Freilich, S., Schuster, S., Milferstedt, K., van der Meer,
668 J.R., Groszkopf, T., Huisman, J., Free, A., Picioreanu, C., Quince, C., Klapper, I.,
669 Labarthe, S., Smets, B.F., Wang, H., Isaac Newton Institute Fellows, Soyer, O.S.,
670 2016. Challenges in microbial ecology: building predictive understanding of
671 community function and dynamics. *ISME J.* 1–12.
672 <https://doi.org/10.1038/ismej.2016.45>
- 673 Xu, R., Yang, Z.H., Zheng, Y., Liu, J.B., Xiong, W.P., Zhang, Y.R., Lu, Y., Xue, W.J.,

- 674 Fan, C.Z., 2018. Organic loading rate and hydraulic retention time shape distinct
675 ecological networks of anaerobic digestion related microbiome. *Bioresour.*
676 *Technol.* 262, 184–193. <https://doi.org/10.1016/j.biortech.2018.04.083>
- 677 Zhang, W., Werner, J.J., Agler, M.T., Angenent, L.T., 2014. Substrate type drives
678 variation in reactor microbiomes of anaerobic digesters. *Bioresour. Technol.* 151,
679 397–401. <https://doi.org/10.1016/j.biortech.2013.10.004>
- 680 Zhou, J., Liu, W., Deng, Y., Jiang, Y.-H., Xue, K., He, Z., Van Nostrand, J.D., Wu, L.,
681 Yang, Y., Wang, A., 2013. Stochastic assembly leads to alternative communities
682 with distinct functions in a bioreactor microbial community. *MBio* 4, e00584–12–
683 e00584–12. <https://doi.org/10.1128/mBio.00584-12>
- 684 Zhou, J., Ning, D., 2017. Stochastic community assembly: Does it matter in microbial
685 ecology? *Microbiol. Mol. Biol. Rev.* 81, 1–32.
686 <https://doi.org/10.1128/MMBR.00002-17>

689 FIGURE CAPTIONS

690 **Fig 1.** Reactors performance during periods 1 and 2 (average values from R1 and R2
691 and standard deviation). A) Organic loading rate (OLR), methane production and biogas
692 composition; B) pH, total and partial alkalinity, C) acetic, propionic, butyric and valeric
693 acid concentrations. In panel C, time is expressed as day - hour of the day.

694 **Fig 2.** Boxplot of community richness and evenness for *Bacteria* and *Archaea* domains
695 during periods 1 and 2. The graphics show the values of the minimum, first quartile,
696 median, third quartile and maximum. The box comprises 50% of the observations and
697 the points are the outlier values.

698 **Fig 3.** Transformed-based Principal Component Analysis (tbPCA) ordination diplot for
699 the bacterial (A) and archaeal (B) communities. The tbPCAs show the microbial
700 community structure at the OTU level for the two anaerobic reactors during period 1
701 and period 2. Labels indicate the time in hours after the beginning of the OLR shock.
702 Labels of samples taken during period 1 have been omitted for clarity. Blue vectors
703 indicate incrementing values of the operational variables that are significantly correlated
704 with community structure (p-value ≤ 0.01).

705 **Fig.4.** Community composition profile at the most detailed taxonomic level available.
706 Relative abundance of the most prevalent taxa (those exceeding 1% in average) in
707 bacterial (A) and archaeal (B) communities in R1 and R2. For period 1, the averaged
708 relative abundances of each taxon are shown (details included in Fig. A1). Period 2 is
709 organized by hours after OLR shock.

710 **Fig 5.** Co-occurrence network of abundant genera (relative abundances $> 0.1\%$)
711 connected by positive interactions ($q \leq 0.05$). The 9 clusters of highly interconnected
712 microorganisms are shown. Node color indicates the cluster affiliation while node shape
713 refers to the domain: circle for *Bacteria* and square for *Archaea*. For taxonomy
714 assignment of nodes see Fig A2.

715 **Fig.6.** Temporal trends during organic overloading of the abundant clusters of co-
716 occurring microorganisms divided by domain. Accumulated relative abundances of
717 bacterial (A), and archaeal (B) organisms. For comparison, average values during period
718 1 are also shown and denoted as time 0 where error bars indicate standard deviations.
719 Clusters were considered as abundant if the total accumulated relative abundance by
720 domain was larger than 5% on any sample.

721 **Fig. 7.** Variation through time of the dominant microorganisms (relative abundances
722 $>1\%$ in any sample) in AD reactors. Microorganisms best taxonomic resolution is

723 indicated on the right, were (A) indicates *Archaea*, (B) *Bacteria* and (un) undetermined
724 when it was not possible to identify the genus. Cluster affiliation of each microorganism
725 is showed on the left column. Time is expressed as day - hour of the day.

ACCEPTED MANUSCRIPT

Table 1. Total COD, OLR, TS and VS values of feedstock used during the stabilization period, period 1 and 2.

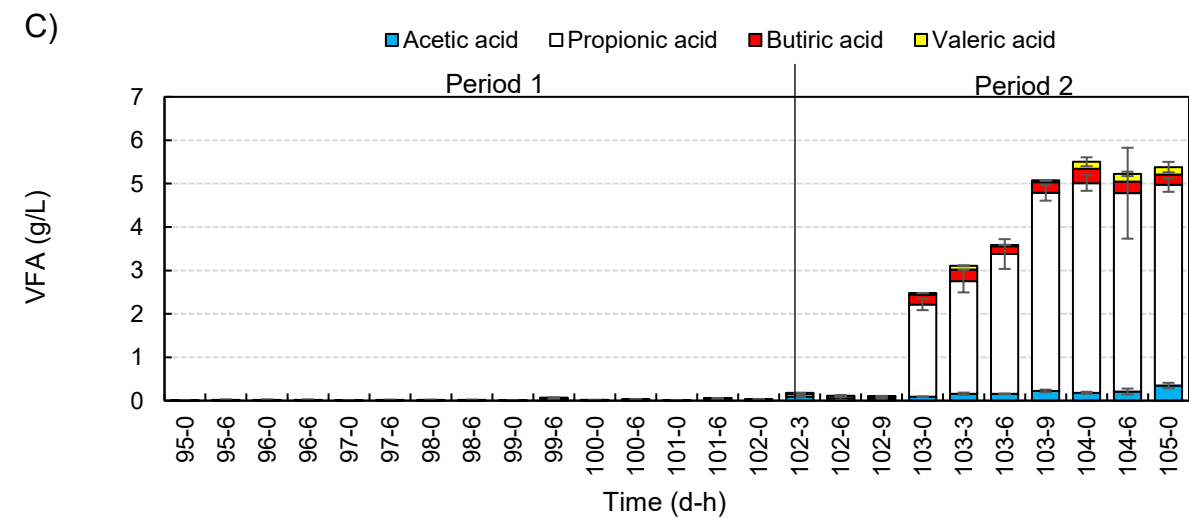
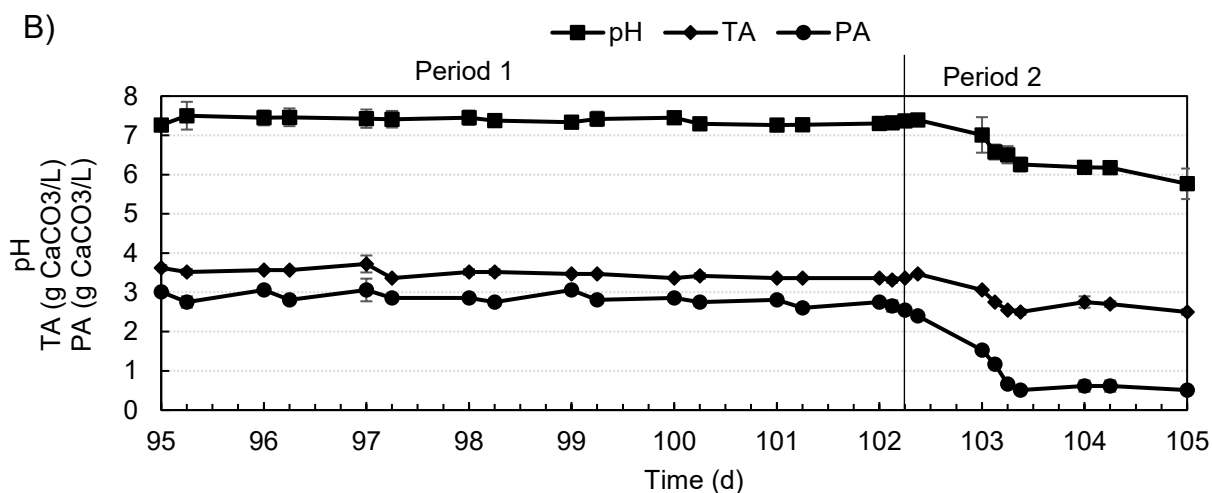
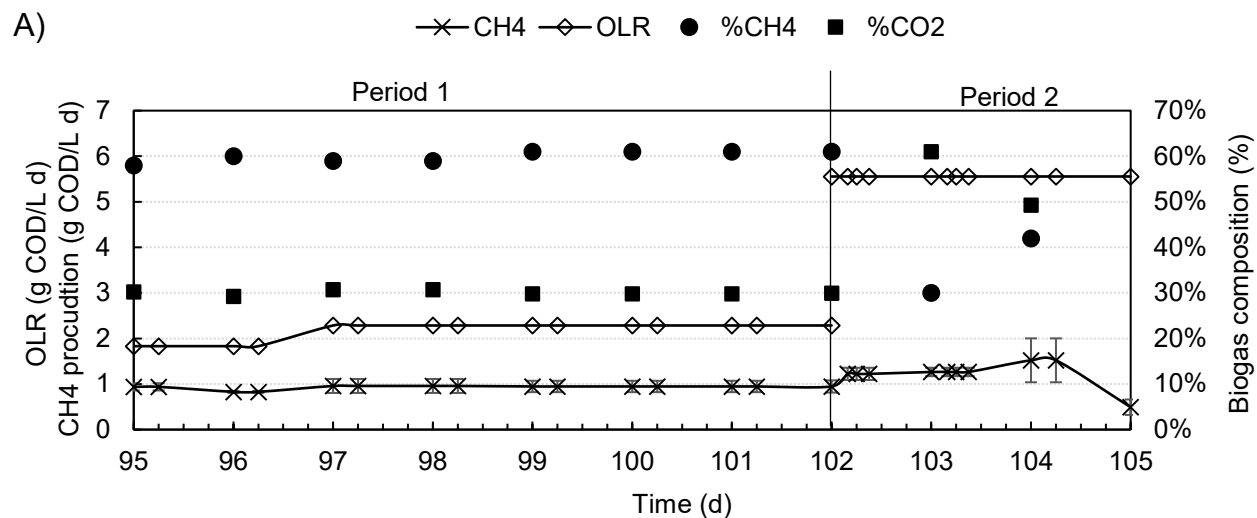
Feedstock characteristics	Stabilization period	Period 1	Period 2
Total COD (g O ₂ /kg)	36.8 ± 0.9	43.1 ± 4.2	111.1 ± 5.3
OLR (g COD/ L d)	1.8 ± 0.1	2.2 ± 0.2	5.6 ± 0.3
TS (g TS/kg)	32.1 ± 0.9	26.6 ± 2.0	74.3 ± 2.1
VS (g TS/kg)	22.8 ± 0.5	21.7 ± 1.6	65.2 ± 1.9

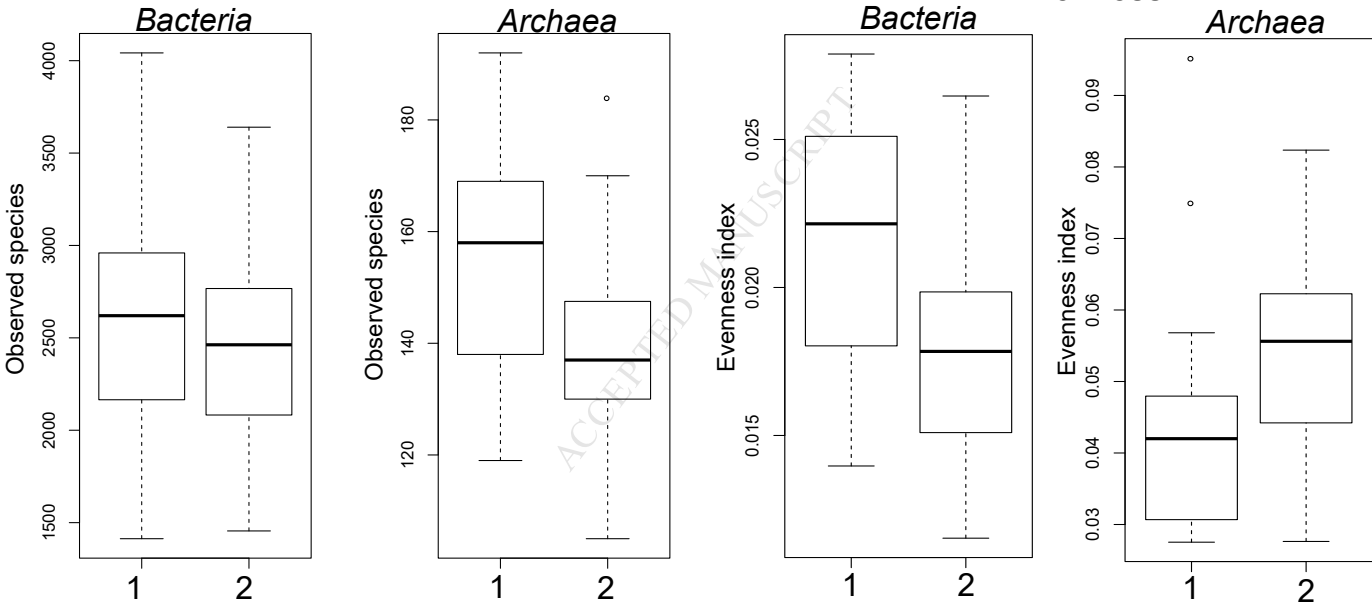
COD: Chemical oxygen demand; OLR: Organic loading rate; TS; Total Solids; VS: volatile solids

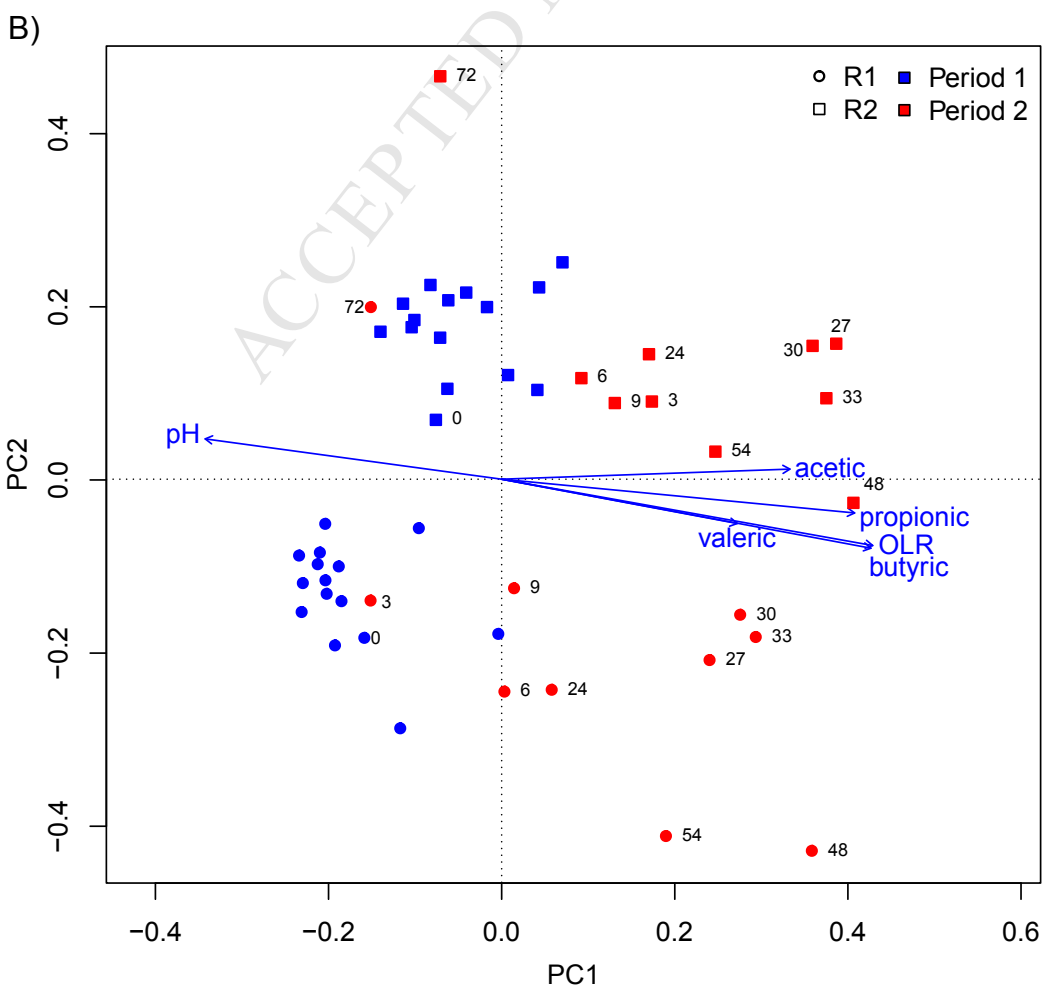
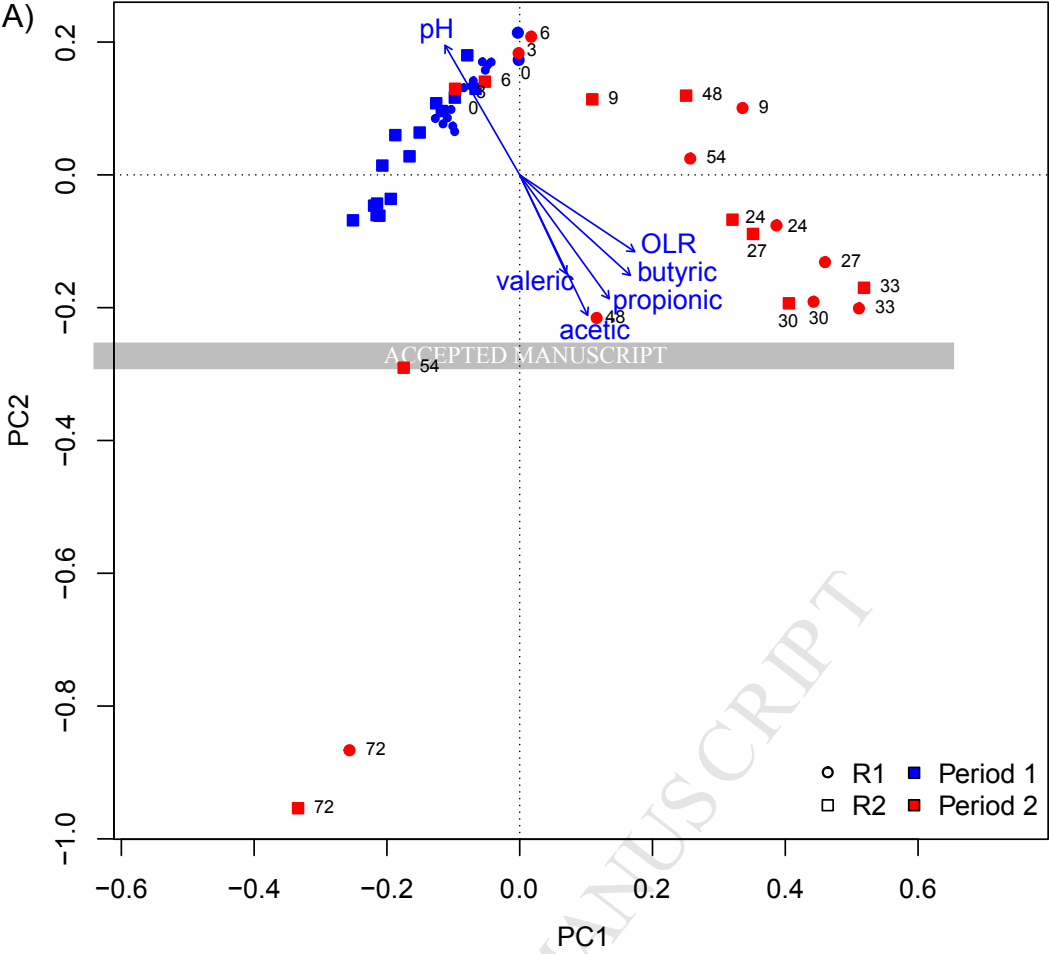
Table 2. Anaerobic reactors performance during stabilization period (days 0-94). Results correspond to averaged values and standard deviations from the two reactors (n = 42).

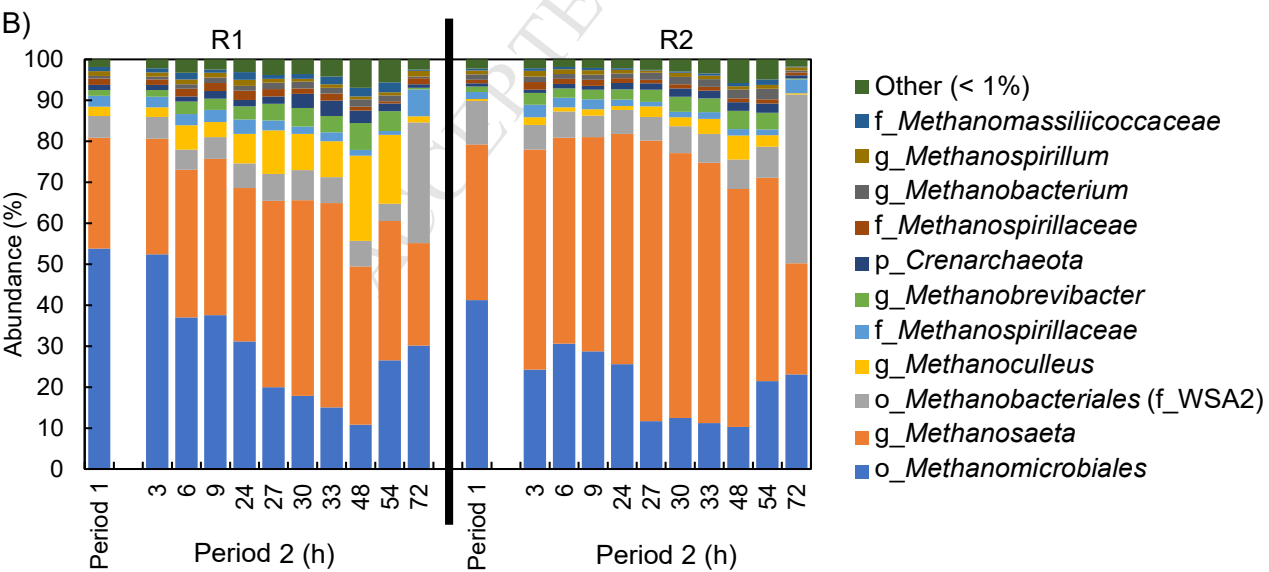
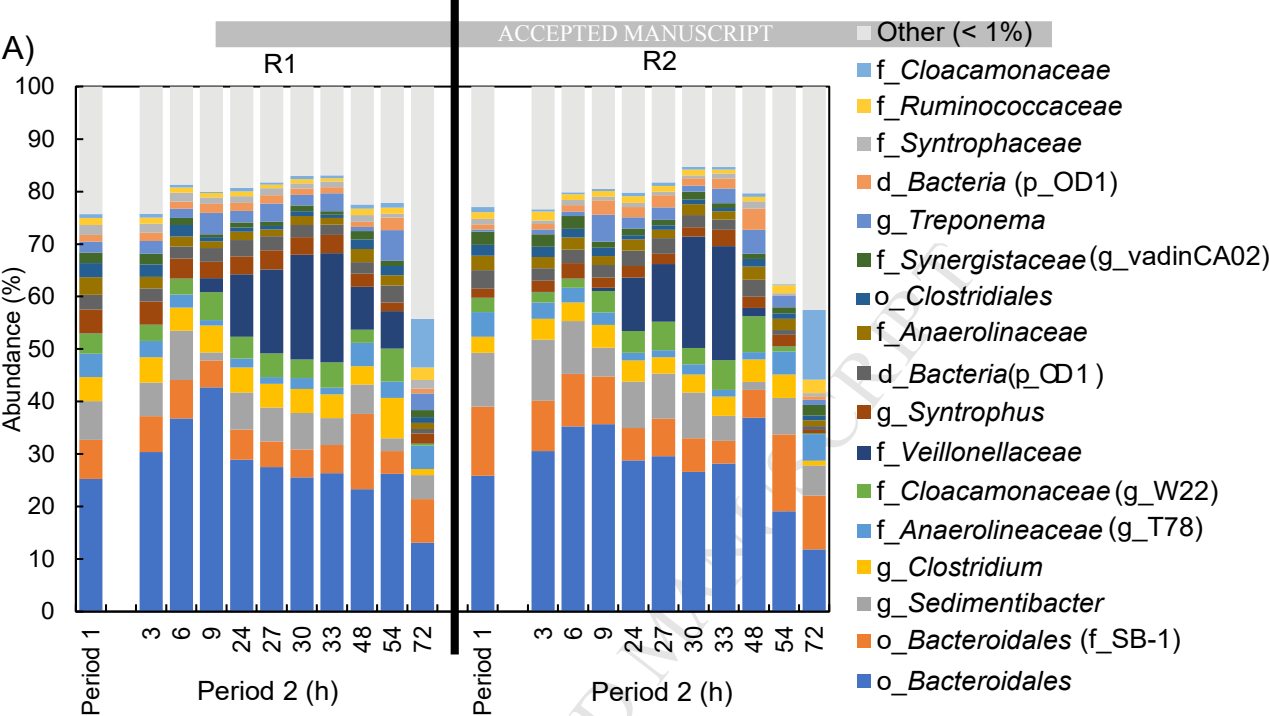
Operational parameters	
OLR (g COD/L d)	1.8 ± 0.1
CH ₄ (g COD/L d)	0.9 ± 0.2
pH	7.3 ± 0.1
TA (g CaCO ₃ /L)	3.6 ± 0.1
PA (g CaCO ₃ /L)	2.8 ± 0.1
TS (g/L)	20.1 ± 3.2
VS (g/L)	10.1 ± 1.1
Acetic acid (mg/L)	< 60
Propionic acid (mg/L)	< 30
Methanization efficiency (%)	45 ± 0.1

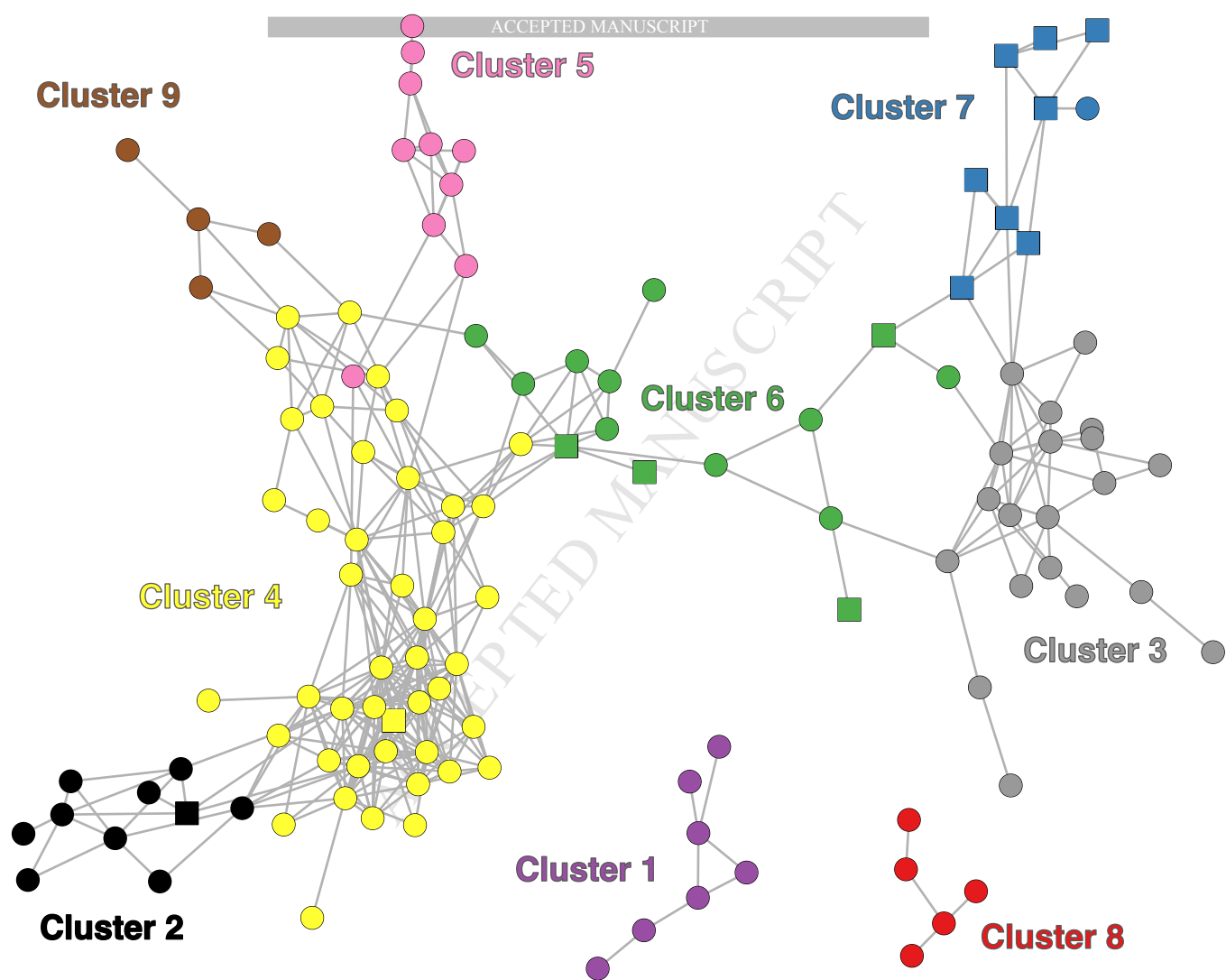
OLR: Organic loading rate; TA: Total alkalinity; PA: Partial alkalinity; TS: Total solids; VS: Volatile solids

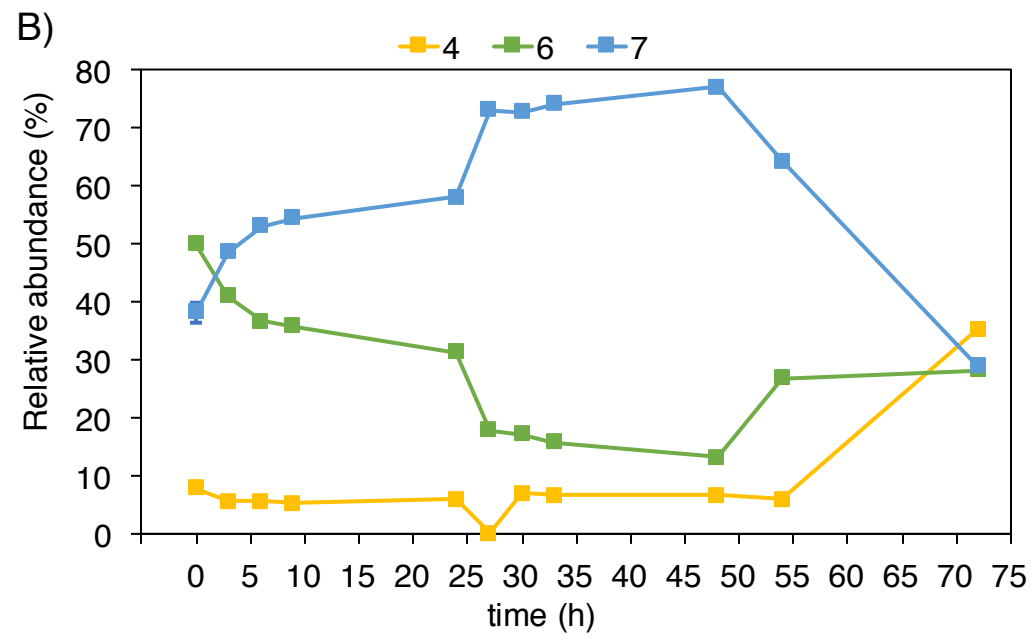
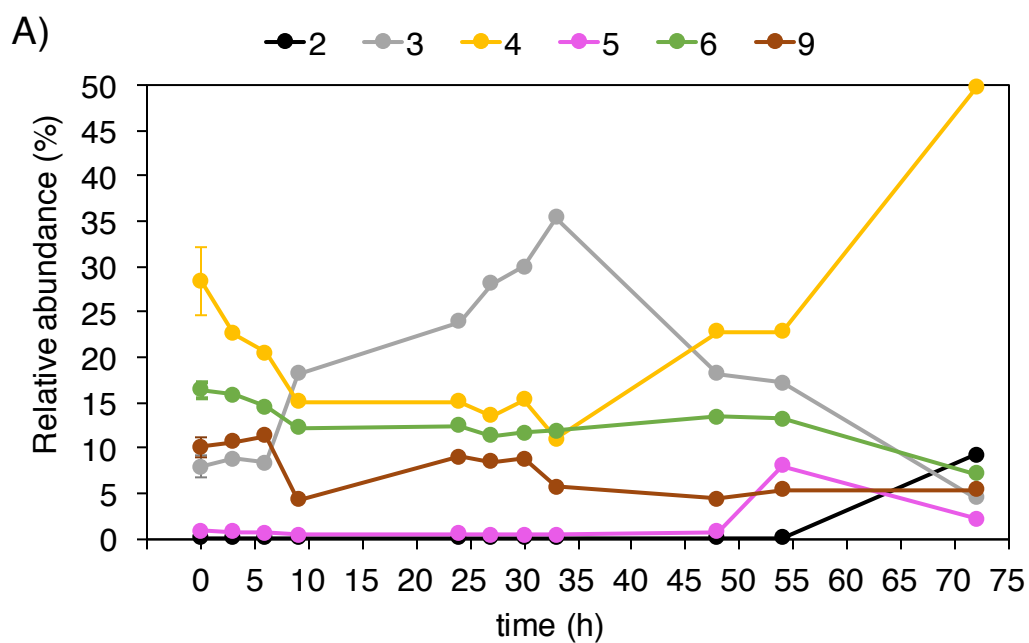












R1

R2

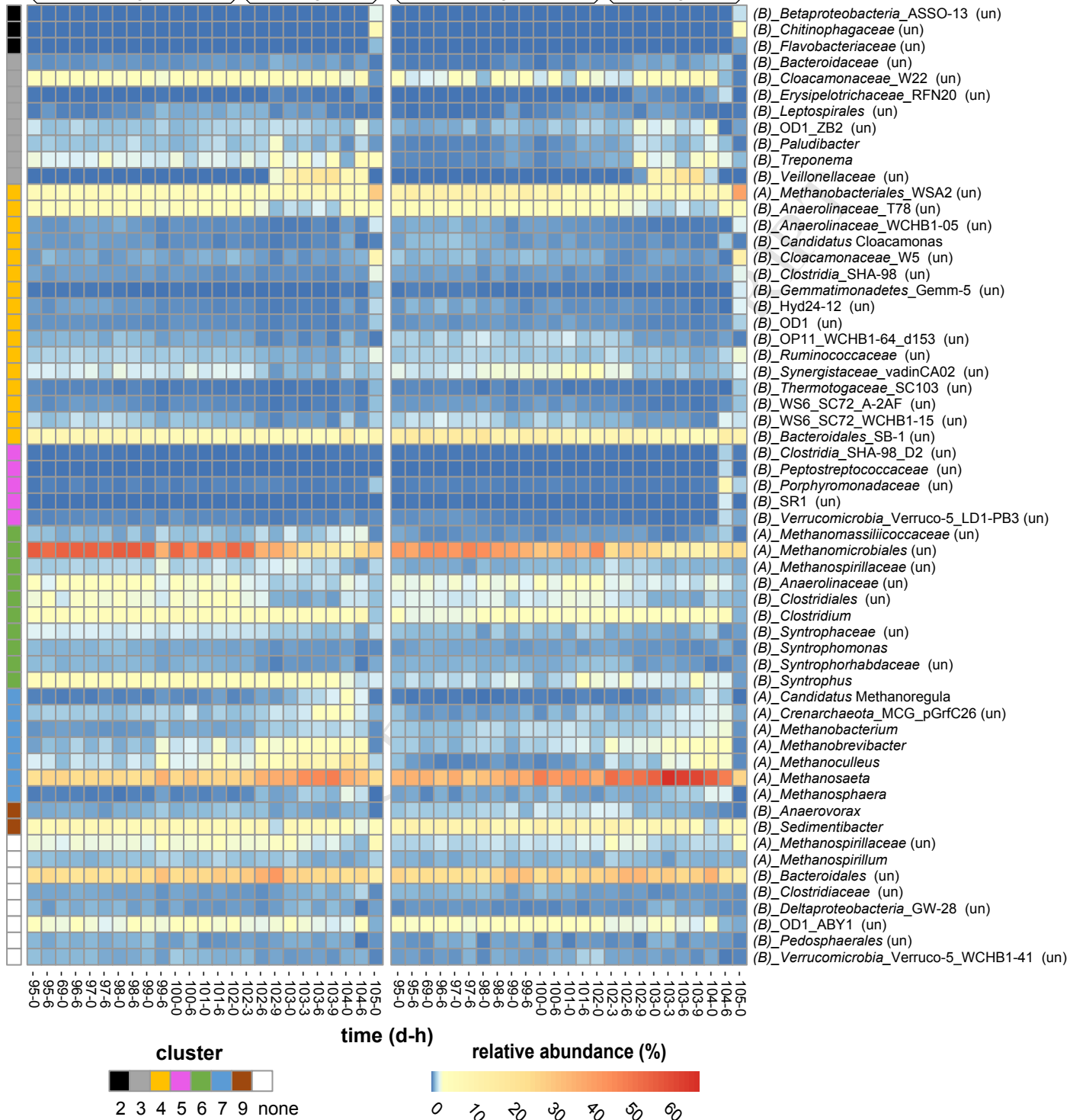
ACQUIRED MANUSCRIPT

PERIOD 1

PERIOD 2

PERIOD 1

PERIOD 2



Highlights

- Operational parameters similarly varied after few hours of organic overloading in replicated reactors.
- *Methanosaeta* sp. incremented with increasing VFA concentrations.
- The organic overloading induced a redistribution in the equitability of microorganisms and a loss of *Archaea* species.
- Community structure was not resilient changing rapidly after the OLR increased.
- Fast temporal replacement of functionally redundant microorganisms was observed.